Non-Destructive Testing Methodology for Impregnation Quality Identification of Segmented Stators in a Traction Motor

Gabriele Piombo[1], Xiyun Ma[1], Simon Guicheteau[2], Juliette Soulard[1]
[1]*Warwick Manufacturing Group, University of Warwick,* Coventry, United Kingdom
[2]*Altair Engineering Ltd.* , Royal Leamington Spa, United Kingdom

***Abstract*—Electrical machines' stator impregnation quality plays a significant role in ensuring optimal system performance by providing electrical insulation, thermal conductivity, and mechanical rigidity. Prior research has established that the thermal DC test is a viable non-invasive technique for discerning the operational and health attributes of electrical machine components, but it is time-consuming. This research aims to investigate the utilization of electrical impedance analysis and derived control variables for the assessment of stator tooth impregnation quality. The research integrates two Type 1 Gauge Repeatability and Reproducibility campaigns to assess the thermal and electrical testing tolerance ranges. The thermal conductance and conductors-to-lamination capacitance measurements performed in an operator-controlled but uncontrolled environment result in a +/-66.7% and +/-4.4% tolerance range, respectively. The greater repeatability of capacitance measurement may lead to an improvement in impregnation quality identification in conditions closer to a production environment. A Finite Element model is leveraged to confirm the hypothesis. Simulation results underline both a strong correlation (ρ=0.99) between thermal conductance and conductor-to-lamination capacitance and their suitability as impregnation goodness diagnostics signals (ρ=0.95, 0.99 respectively). Impedance analysis could have various applications such as identifying defects during manufacturing, or optimizing the impregnation process, reducing part scraping.**

Keywords*—*Impedance Analysis, Impregnation Quality, Non-Destructive Testing, Stator Winding Insulation, Thermal Conductance.

I. Introduction

The efficiency and lifetime of an electric machine (EM) are significantly constrained by its operating temperature. For a traction motor, the continuous performance at a lower speed is limited by stator winding temperature due to high copper losses. Insulation grade determines the maximum temperature that the stator winding can reach. The insulation systems and impregnation process utilised in EMs are identified as the primary factors that enable high efficiency and durability [1].

The primary constituents of the insulation system include a coating encasing each conductor, slot liners and resin that occupies the gaps within the slots. The resin is inserted after the slot liner and winding conductors in a procedure commonly referred to as impregnation. This procedure not only enhances the thermal performance of the stator but also enhances its mechanical robustness through the adhesion of conductors preventing fretting and reinforcing their electrical insulation. The primary techniques employed for impregnation include trickling, roll dipping, hot dipping, vertical dipping, and vacuum pressure impregnation (VPI). Trickle impregnation has been identified as a cost-effective and time-efficient method for high-scale applications [2]. However, it is important to note that this method may result in lower quality and consistency as compared to VPI [3]. Due to imperfections in the impregnation process, residual air may persist within the winding. The introduction of the impregnation goodness (IG) factor in [3] was a coherent approach to precisely model the temperature distribution of the coil. The term "IG" refers to the ratio of resin to air that is present in the slots' gaps on a global scale, and its values range from 0 to 1. In these investigations, distinct variations in IG could be observed in two specific regions of the tooth, namely the liner-lamination (IG_{LL}) and active

Author's version of article accepted for publication on 30th September 2023.
G. Piombo, X.Y. Ma, S. Guicheteau, J. Soulard, 'Non-Destructive Testing Methodology for Impregnation Quality Identification of Segmented Stators in a Traction Motor', 2023 IEEE Transportation Electrification Conference & Expo (ITEC) Asia-Pacific, Chiang Mai, Thailand.
The investigations were supported by the Engineering Centre for Doctoral Training in Sustainable Materials and Manufacturing (grant number: EP/L016389/1) complemented by funding from Altair Engineering Ltd. (UK).

winding (IG_{AW}) zones. The values of IG_{LL} are typically lower than IG_{AW} due to the hindrance caused by the slot liner to the diffusion of resin between the winding and the laminations [1].

Insulation materials, conductor placement in slots and impregnation quality influence the behaviour of the wound teeth. To meet production requirements, it is therefore crucial to ensure EoLine methods are sensitive to these variables. EoLine impregnation tests include running thermal, DC Hipot, and surge tests. EoLine tests after significant manufacturing stages have been performed and all likely production line problems have accumulated raising the difficulty of identifying flaws [4]. At this level, errors can only be fixed by time-consuming rework or demolition, at the cost of machining time, material and energy [5]. The insulation system and impregnation quality have an impact not only on the manufacturing scrap and performance but also on the durability of the machine. EMs insulation systems age from exposure to different temperatures, mechanical vibrations and atmospheric conditions over many years of operation [6]. Thus, EMs must be monitored for initial IG and insulation ageing over several years. While thermal tests have been used to detect the first, electrical tests have been used to identify the latter.

According to winding insulation health and degradation literature, IG affects capacitance between conductor-to-conductor (C-C) and conductor-to-lamination (C-L) in stator teeth, thermal properties, and high-frequency responsiveness to external electric stress sources. Therefore, if defects in terms of air inclusion in the resin are present, capacitance would manifest a variation and its identification could inform about IG. There is no conclusive study on how to measure impregnation quality and its effects on electric variables. The first step to identifying the applicability of electrical testing as a means of IG qualification consists of the assessment of the two competing measurement techniques' repeatability and reproducibility. This research extends previous investigations by adding operator-induced variability to Gauge R&R investigations of motorette thermal characterization. The Gauge R&R procedure for tolerance detection on impedance analysis as electrical testing is the second step before comparing the two methodologies and estimating the level of correlation between the results. The aim is to identify IG in absolute value but a reliable quantification of variability in production would also prove useful.

This paper is organised into six sections. Section II presents the state-of-the-art in Non-Destructive Test (NDT) methods for impregnation quality identification, including stator tooth thermal and electrical characterization methods and their limitations. Section III summarises the two experimental procedures pursued. Section IV describes the modelling methodology using 2D Finite Element (FE) and the simulated space. Section V provides an overview of the findings with an emphasis on testing methodologies assessment based on the thermal steady-state and electro-static simulation results. In section VI, conclusions are drawn.

II. Non-destructive test methods for impregnation quality identification

Previous studies attempted to identify the IG via thermal test procedures as air inclusion impacts the thermal conductivity and specific heat capacity of the stator tooth. Reference [7] proposed a methodology for characterising the winding bulk thermal steady-state and transient properties. The authors experimentally validated an analytical and FE considering resin heat capacity and weight, which affect model accuracy under dynamic conditions. The proposed technique overcomes the need to introduce a novel lumped parameters model by creating an equivalent impregnation-conductor material, which limits thermal model calibration efforts. Motorette testing was proven an efficient experimental method to characterise EMs thermal performance by determining stator section parameters [8].

In [9], a time-efficient motorette testing setup has been developed and used to determine 264 stator segments' thermal parameters, allowing the assessment of winding and impregnation production processes. Test time was reduced to 10 minutes and its rapidity was leveraged to modify impregnation settings and determine process elements that affect wound tooth thermal conductance. The +/-6.3% tolerance range of the testing procedure was identified via single operator Gauge Repeatability and Reproducibility (R&R) methodology. The test was performed in a controlled environment, insulating the equipment to reduce external influences. Although fast when compared to previous thermal characterisation attempts, the available IG test procedures are still slower than electrical testing alternatives. The measurements' repeatability in a production-alike environment may be compromised by mounting the part on the radiator (operator) and the need to control the heat exchange of the part with ambient air.

Pulse Width Modulation (PWM) inverters' steep-fronted pulses cause quick transient over-voltages that stress the electrical insulation system and promote State-of-Health (SoH) deterioration [10]. Each turn-to-turn and primary insulation has capacitance and resistance to the stator core and other coil and winding turns [6]. Several studies have examined capacitance measurements as health diagnostic indicators, while others highlighted its hazards owing to measurement uncertainty [11]. The utilisation of turn-to-turn capacitance for insulation deterioration monitoring is employed in [12] under the rationale that insulation system SoH evolution influences winding frequency resonances at high frequency. A stator conductor to grounded core equivalent capacitance (C_{eq}) test is established in [13] to detect insulation problems. The C_{eq} tracking is suggested to indicate insulation issues such as moisture absorption, thermal degeneration, and end winding contamination. Reference [14] found that strand-to-strand Insulation Capacitance (IC) is correlated with thermal exposure duration and thermal ageing accumulation after 1200 hours of testing. Identifying strand-to-strand IC as an indicator of thermal ageing qualities is suggested to reduce EMs thermal qualification time and speed up prototyping. Similar results are obtained in [15], [16]. Although confirmed, the relationship between capacitance and ageing is inferred to be difficult to identify without considering temperature influence. EMs' available Current Transformers (CTs) are used in [17] to monitor ground IC changes utilising peak terminal voltage and leakage currents. IC is reported to decrease with thermal ageing and increase with end-winding contamination. Among the other methods, offline component quality inspections during production and cyclic EM ageing monitoring rely on impedance analysis, which has the potential to early detect ground-wall insulation issues. Alternatively, by injecting a small High-Frequency (HF) signal close to the resonance frequency into the stator winding, non-intrusive condition monitoring can be used to analyse the SoH of insulation during operation [18]. The approach detects minor variations in the stator winding's turn-to-turn capacitance to monitor the insulation's degeneration. This approach is suitable for online state monitoring. Nevertheless, its accuracy is lower than offline methods. IEEE & IEC standards already implement capacitance-related testing for EM inspection, repair and rewind, but no current procedure is in place for tracking impregnation quality [19].

III. Experimental Setup

The experimental campaigns in this study rely on the utilisation of a Type 1 Gauge R&R methodology. First, previously published motorette setup reliability for tooth impregnation thermal conductance identification is analyzed. Second, the repeatability and reproducibility of capturing C-C and C-L electrical properties using a calibrated Wayne Kerr 6500B impedance analyzer are investigated.

Details of the motorette testing equipment are presented in [9]. The thermal tests setup includes a control unit (CU), power cables, chiller, cooling pipes and plate, and two T-type thermocouples, as included in Fig. 1. The safety Plexiglas box is a modification to the set-up in [9], which used insulating foam to limit air convection at the surfaces of the wound tooth not in contact with the radiator. The CU minimizes the test time to reach a thermal steady-state via a closed-loop temperature control logic the first minute via constant current, then switching to constant voltage to prevent overshooting. The target temperature is set at 70°C to reduce signal dependency to thermocouple accuracy. The steady state is considered reached once the temperature fluctuation is less than 1°C in the previous 10 minutes. The two T-type thermocouples monitor both the temperature of the tooth surface in contact with the cooling plate ($T_{Cooling\ Plate}$) and the winding's outer surface temperature ($T_{Windings}$). Knowing the CU input power, the thermal conductance can then be calculated as:

$$\mathrm{TC} = \frac{V_{CU} I_{CU}}{T_{Windings} - T_{Cooling\ Plate}} \tag{1}$$

Where TC is the global sample thermal conductance in W/K, V_{CU} and I_{CU} are the control voltage and current, respectively.

The electrical testing setup consists of a calibrated 6500B Wayne Kerr impedance analyzer and sensing cables and clips. Parallel and series circuit configurations are tested in ambient conditions to gather samples' conductor-to-conductor and conductors-to-lamination properties, respectively, as reported in Fig. 2. The selected frequency range is 100kHz to 2MHz with a slow speed setting for increased accuracy.

Experimental results for both test methods are presented in section V.A.

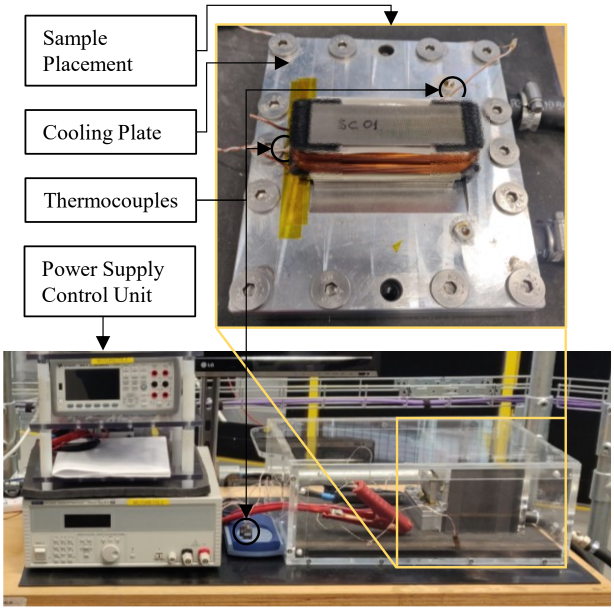

Fig. 2. DC thermal test experimental rig. Detail of the sample placement location (top) and overview of the testing equipment (bottom).

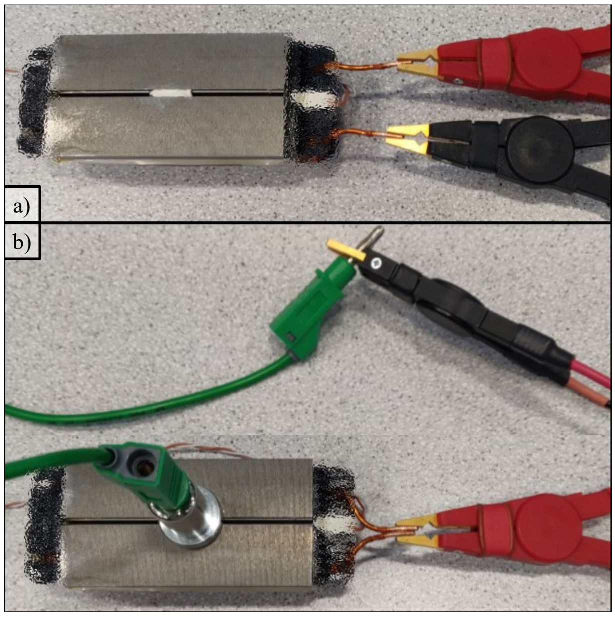

Fig. 1. Overview of the electrical testing setup with a) conductor-to-conductor (C-C) and b) conductors-to-lamination (C-L) connection configurations.

IV. Modelling

A Finite Element Method (FEM) based model is developed in an Altair® Flux® environment. Well-established FE methodology allows a comprehensive and reliable representation of the segmented stator tooth thermal and electrical characteristics. The geometry of the tooth is shown in Fig. 3. The different parts include lamination, slot wedge, windings, insulation, slot liner, and impregnation resin. Four model areas where resin is inserted are added to the FE model to isolate their contribution to the overall component performance. These consist of the airgap between the slot liner and the lamination (AG) and areas extending from the upper part of the liner to the top-left corner of the part (Inner), the outer side (Outer), and spaces among the windings (Central). Each of the specific areas is given an impregnation goodness (IG) value ranging from 0 to 1, representing the resin-impregnated coverage to total available area ratio. The central area's impregnation goodness is fixed to a constant value of 1 during simulations. This is due to previous findings identifying critical areas for resin inclusion are inner, outer and airgap, while the space among conductors resulted in being more evenly filled [1]. A global IG parameter is calculated as follows:

$$Global\ IG = \frac{Area_{Resin}}{Area_{Total}} = \frac{A_{IN}IG_{IN} + A_{OUT}IG_{OUT} + A_{AG}IG_{AG} + A_{CEN}IG_{CEN}}{A_{IN}+A_{OUT}+A_{AG} + A_{CEN}} \quad (2)$$

where A_{IN}, A_{OUT}, A_{AG}, A_{CEN} and IG_{IN}, IG_{OUT}, IG_{AG}, IG_{CEN} are the inner, outer, airgap and central areas in m^2 and impregnation goodness values, respectively. A list of the parameters included in the study to fully represent the sample geometry is included in Table II, together with their set values, units and acronyms depicted in Fig. 3. FEM simulations necessitate a set of input parameters and boundary conditions to be effective and representative of real-world scenarios. Three input variables are included as listed in Table III, indicated as the IG in inner, outer and airgap areas (IG_{IN}, IG_{OUT} and IG_{AG}, respectively). To ensure the simulated space does not exceed the geometric boundaries of the part, a constraint is imposed on the GTB-MWY relationship as follows:

$$-0.55 + \mathrm{INS} + \mathrm{GTB} \leq \mathrm{MWY} \leq 0.7 \quad (3)$$

TABLE I. MATERIAL TYPES OF THE SEGMENTED STATOR PARTS

Component	Material	Thermal Conductivity [W/m/K]	Relative permittivity ε_r [-]
Lamination	M270-35A	25	-
Windings	Copper	398	-
Airgap	Air	0.025	1
Wire insulation	-	0.21	3.9
Slot liner	PEEK	0.25	3.5
Slot wedge	Plastic	0.7	-
Impregnation	Resin	0.2	2.5

TABLE II. FIXED GEOMETRIC PARAMETERS OF THE FEM MODEL

Parameter	Abbrev.	Value [mm]
Gap Inner	GI	0.1
Gap Outer	GO	0.1
Gap Tooth 1	GT1	0.1
Gap Tooth 2	GT2	GT1
Insulation	INS	0.1
Move Wires X	MWX	0.05
Tooth Gap Width 1	TW1	4
Tooth Gap Width 2	TW2	4
Gap Tooth Base	GTB	0.1
Move Wires Y	MWY	0

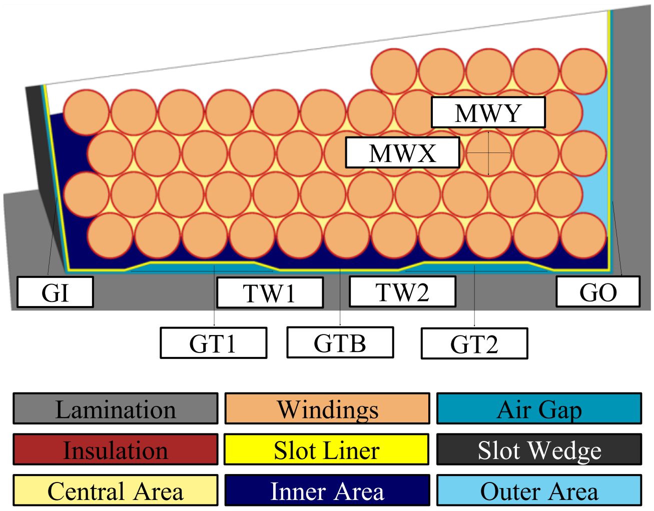

Fig. 3: FEM model geometry, designed impregnation areas and geometric parameter implemented in the simulations. Reference to the parameters values is offered in Table II and Table III.

TABLE III. SIMULATION PARAMETER RANGES

Parameter	Abbrev.	Range	Unit
Inner Area IG	IG_{IN}	0.1-1.0	[-]
Outer Area IG	IG_{OUT}	0.1-1.0	[-]
Airgap Area IG	IG_{AG}	0.1-1.0	[-]

The constraint imposed in (3) is fully respected in the space simulated in this study. Two types of Flux® applications are simulated on the depicted geometry, namely thermal and electro-static. The first application calculates the steady state temperature reached by the part starting at 23°C ambient conditions under experimental campaign-derived end-of-test power supply (17W) and fixed cooling plate temperature (26°C) via fundamental heat conduction equations. Each material representation incorporates thermal and electrical properties based on an extensive literature review and preliminary campaigns as reported in Table I. Relevant to the calculations, epoxy resin thermal conductivity and relative permittivity (ε_r) properties are set to 0.2 [W/m/K] and 2.5 [-], respectively. The global thermal conductance between two temperature sensors' representing the actual locations of the thermocouples installed in the tested sample can then be obtained by leveraging (1).

The second application calculates the electric energy content of the system when a unitary voltage difference is imposed between conductors and lamination. The conductors-to-lamination capacitance ($Cap._{(C\text{-}L)}$) can then be calculated as:

$$W_e = \frac{1}{2} Cap._{(C-L)} U^2 \rightarrow Cap._{(C-L)} = \frac{2W_e}{U^2} \quad (4)$$

where W_e is the electrostatic energy for a linear and isotropic medium in the considered volume and U is the potential difference between the conductors.

V. RESULTS AND DISCUSSION

A. *Type 1 Gauge R&R experimental results*

In [9], 30 repetitive thermal tests are reported following a Type 1 Gauge R&R procedure in an insulated environment. The emerging tolerance of thermal conductance is +/- 6.3%. The authors recommended assessing the error range of the motorette setup before performing a series of tests. This paper coherently extends the previous efforts at assessing motorette measurement tolerances. Type 1 Gauge R&R methodology is not capable of isolating operator, part, and repeatability contributions to the results to the same extent as a complete gauge R&R including types 2 and 3. Nevertheless, it has the benefit of not requiring multiple operators but still maintaining rigorousness in statistically identifying the tolerance range of the measurement. An added layer of confidence is represented by testing 2 parts and introducing an additional operator as in the case of this study. The whole testing procedure is repeated 30 times, including setup preparation, parts insertion, test execution, connections teardown and data extraction. The test execution time is 12 minutes, plus 5 minutes for setup assembly, 3 minutes for dismantling and 10 minutes for cool-down, on average.

The Gauge R&R test results are reported in Fig. 4 and Fig. 5. The tolerance range value is based on a capability of the gauge value of 1.33 and 6 standard deviations that represent the entire process spread, resulting in a confidence of 99.7%. If the capability of the gauge is greater than the set 1.33 threshold, the experimental setup can measure parts consistently within the resulting tolerance range. The motorette tolerance results in +/- 66.7%. The reasons for the order of degree of difference when compared to the previous studies are multiple. The previously run Type 1 Gauge R&R did not include the operators' contribution to errors as the part was not removed and replaced on the radiator. Most importantly, the test setup is not insulated in the same way in this study to extend the repeatability results to conditions closer to the targeted manufacturing application where parts measured in the open air within an enclosure would be preferable. The difference in the order of magnitude of tolerance could therefore be primarily attributable to these differences. A higher target temperature than 70°C may potentially mitigate this effect by reducing the thermocouples' tolerance impact on the measurements but it would lead to a longer test time. Last, the next experiments will address the setup mounting and dismantling stages to limit the complexity, improve the test repeatability across operators and most importantly control the natural convection heat transfer.

The second experimental procedure under review is the impedance analysis. The capacitance between the conductor to conductor (C-C) and the capacitance between the conductor and lamination (C-L) can be measured via the connections shown in Fig. 2 a) and b), respectively. The same segmented tooth with concentrated winding has been tested a total of 30 times in line with the motorette evaluation procedure. In the case of impedance analysis, the placement of the tooth, clip connection, machine test type selection and data extraction are the steps involved in the repeatability study. The test time is divided into 1 minute for the tooth placement, 30 seconds for the test execution, 30 seconds for the connections dismantling and 30 seconds for the data extraction, all steps requiring manual intervention.

Table IV summarises the mean investigation results across the parts for the considered electrical properties. The C-L capacitance resulted in +/- 4.4% tolerance as reported in Fig. 5, while the deviation of the C-C capacitance is +/- 9.2%. Other electrical properties such as resonance frequency, resistance and inductance resulted in lower tolerances, which are +/- 3.6%, 3.1% and 7.4% respectively. All the tolerances resulted in the same order of magnitude.

The two capacitances emerged from the literature as indicators of the SoH of the insulation system, for the global SoH of the winding insulation (C-C) and placement of conductor, and the amount of air bubbles inclusion in the gaps between conductors and stator core (C-L), respectively. The latter resulted in having strong repeatability from the tests so it is the subject of the simulations presented in the remaining part of this study.

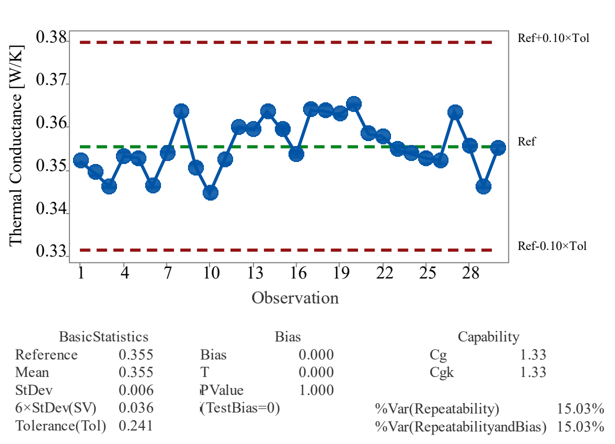

Fig. 5. Type 1 Gauge R&R study of thermal conductance.

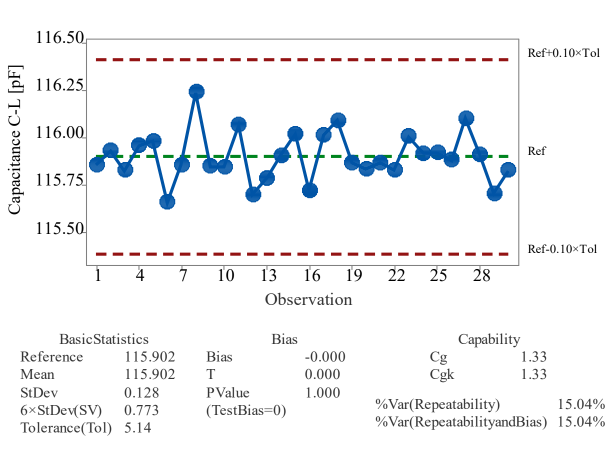

Fig. 4. Type 1 Gauge R&R study of conductor-to-lamination capacitance.

TABLE IV. TYPE 1 GAUGE R&R STUDY SUMMARIZED RESULTS

	Motorette	Impedance analysis (Series connected)	Impedance analysis (Parallel connected)			
	Th. Cond. [W/K]	C-L Cap. [pF]	Resonant Freq. [kHz]	Resistance [kΩ]	C-C Cap. [pF]	Ind. [μH]
Std	0.01	0.13	0.63	0.01	0.29	0.78
Mean	0.36	115.90	698.25	11.34	124.46	417.64
Tolerance [+/- %]	66.7	4.4	3.6	3.1	9.2	7.4

When comparing the two tests' Gauge R&R results, it is evident the advantage of impedance analysis to motorette testing both in terms of repeatability and execution times when the environmental conditions of the part quality test cannot be strictly controlled.

B. FEM model simulations

The development of the FEM model is aimed at an early understanding of potential relationships between wound tooth thermal conductance, conductor-to-lamination capacitance, and impregnation goodness. This is achieved by comparing the results of thermal and electro-static applications. The same model undergoes 50 simulations, outputting the three key indicators presented in Fig. 6.

Fig. 6 is composed of different graph types. Fig. 6 a), b) and c) are the scatter plots representing the indicators' relative distributions and correlations via Pearson coefficients (ρ). The simulation results provide valuable insights into the assessment of the impregnation quality of segmented stators. It can be observed in Fig. 6 a), b) and c) that as the IG deteriorates, there is a corresponding decrease in both the thermal conductance and conductor-to-lamination capacitance. This is confirmed by the positive correlation coefficients of 99%, 97% and 99% between TC and Cap. C-L, TC and Global IG, and Cap. C-L and Global IG, respectively. The shapes of the scattered points evidence the uniformity and strong linearity of the relationship among the evaluated features, which are distributed close to the green linear regression lines.

Fig. 6 d), e) and f) are the Pareto Plots, where each bar indicates the individual contribution of an input variable to the TC, Cap. C-L and Global IG values, respectively. This plot is useful in identifying if any input variable has a larger impact on the responses when compared to the remaining ones. In this study, the three indicators are influenced in an equal manner by the considered variables. This means that the same strategy could ideally be put in place for the three responses. It stands out from the absolute contributions that the primary area requiring attention is the inner, followed by the airgap and the outer ones. The Pareto plots indicate that the greatest contribution would be made by improving the impregnation quality in the inner area. In the thermal application of Fig. 6 d), this is physically justified by the heat flux lines' directions, which are perpendicular to the slot liner when exiting the active area towards the lamination. Better thermal properties of the airgap and inner areas would impact the steady-state temperature more than a higher quality in the outer area. On the other hand, in the electro-static application reported in Fig. 6 e), capacitance is directly proportional to the electrostatic force field between the conductors and the laminated steel, hence a higher quantity of air in the space between them reduces the capacitance value as shown by the correlation lines in Fig. 6 c). The impregnation quality of the outer area has the lowest influence on both the thermal and electrical indicators. Its limited area but principally its location away from the main heat flux or electric field are conducive to a low impact of this region on the part's characteristics. As expected, the Global IG is dependent on the impregnation quality in the three regions included in the simulation inputs. The ranking of Fig. 6 f) is in this case dependent on the area occupied by each region and can therefore be trivially justified.

On the diagonal, Fig. 6 g), h) and i) represent the distribution of the observations in the evaluated simulation results via kernel density estimate (KDE) plots. This plot presents the observations using a continuous probability density curve. It is included as it can inform about any bias in the evaluated space. In this case, the curves indicate the entirety of the targeted space has been uniformly investigated, with no peaks which would have indicated a bias in the distribution of the outputs.

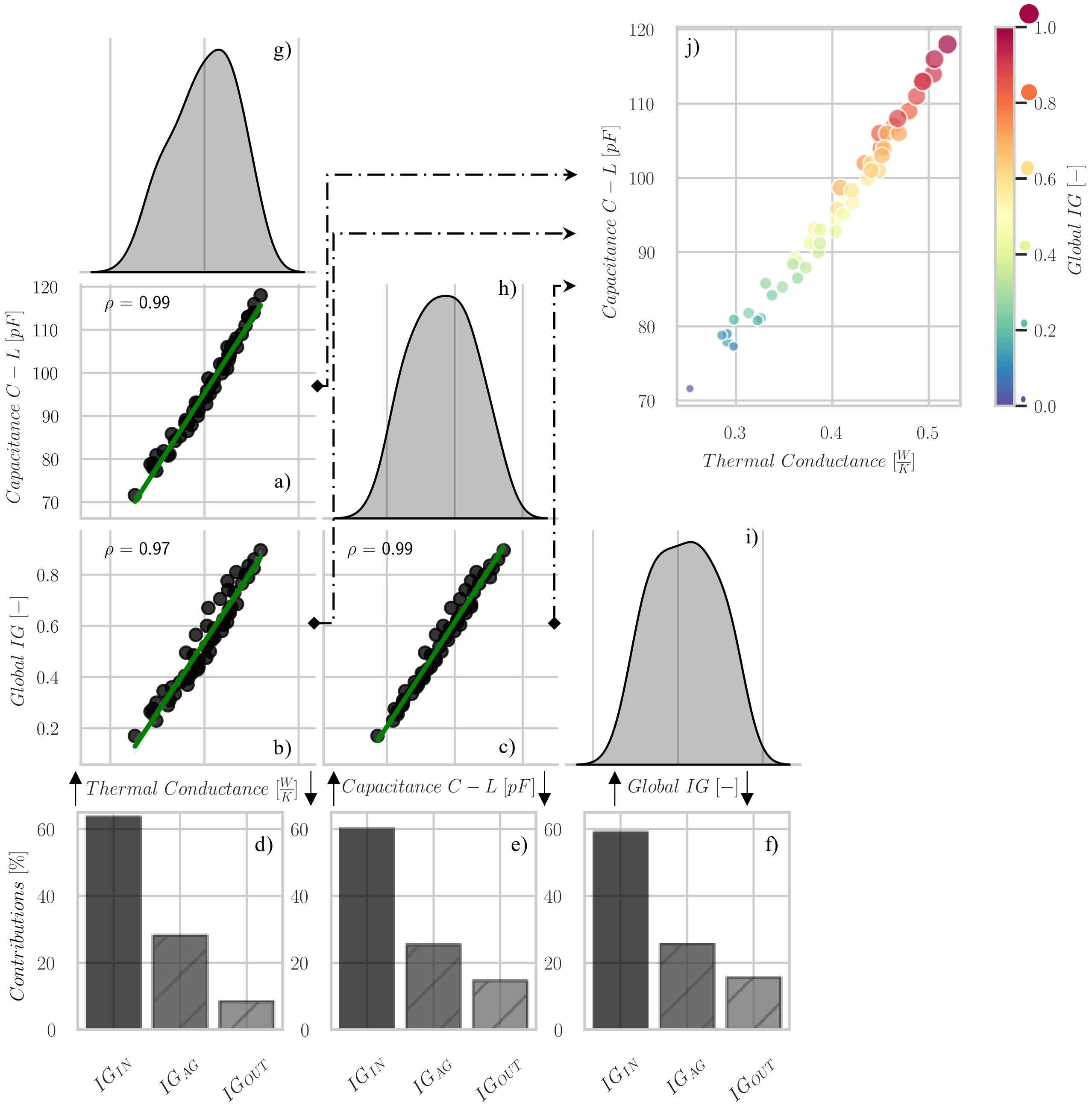

Fig. 6. FEM model simulation results. (a, b, c) Scatter plots of the relationship among Global Impregnation Goodness, Thermal Conductance and Conductors-to-Lamination Capacitance results, with Pearson correlation coefficient (ρ) in the top left corner and overlayed linear regression lines. (d, e, f) Pareto plots of the impregnated areas individual contributions to the responses. (g, h, i) Kernel Density Estimate plots of the targeted responses in the simulated space. (j) Simulation results scatter plot of the relative relationship among Global IG, TC and Cap. C-L.

Last, in Fig. 6 j), the black scatter plot of subplot a) is re-designed to include the visualization of the contribution of Global IG in the relationship between TC and Cap. C-L. This graph is a strong indicator of the interchangeability of the TC and Cap. C-L as an assessment metric of Global IG and can be used to infer the suitability of a sensing choice depending on the application requirements.

VI. Conclusions

The simulation outputs of the developed segmented stator tooth FEM model offered valuable insights into the influence of air inclusion in different areas of the slot in the impregnation process. An increase in impregnation goodness is directly reflected in an increase in the thermal conductance and conductors-to-lamination capacitance. These results suggest the suitability of electrical testing as a strong impregnation quality assessment tool.

Upon experimental validation, these results are expected to be of primary importance for helping in the early detection of stator segment defects. Implementing impedance analysis on tooth coils in the manufacturing line may improve the process optimization degrees of freedom by introducing selection logic limiting the radial temperature differences in assembled segmented stators. This may then translate into higher safety standards during operation, longer machine lifetime, lower maintenance cost and lower manufacturing scrap.

The next steps will include the experimental verification of the correlations between the thermal and electrical features on different sample batches including geometric variations of the segmented stator tooth due to manufacturing inconsistency, once the repeatability of the thermal DC test has been improved by controlling the natural air convection around the part under test.

Acknowledgment

The research outlined in this manuscript is supported by Altair Engineering (UK) Limited via the Engineering Centre for Doctoral Training in Sustainable Materials and Manufacturing (grant number: EP/L016389/1)

References

[1] Y. Guo, J. Soulard, and D. Greenwood, "Challenges in Electric Machine Stator Manufacturing and Their Influences on Thermal Performance," in *2019 9th International Electric Drives Production Conference (EDPC)*, 2019, pp. 1–9, doi: 10.1109/EDPC48408.2019.9011826.

[2] C. E. Thurman, "Trickle Impregnation Of Small Motors," *IEEE Electr. Insul. Mag.*, vol. 5, no. 3, pp. 30–35, May 1989, doi: 10.1109/57.32447.

[3] A. Boglietti, A. Cavagnino, and D. Staton, "Determination of Critical Parameters in Electrical Machine Thermal Models," *IEEE Trans. Ind. Appl.*, vol. 44, no. 4, pp. 1150–1159, 2008, doi: 10.1109/TIA.2008.926233.

[4] Q. Huang, S. Zhou, and J. Shi, "Diagnosis of Multi-Operational Machining Processes Through Variation Propagation Analysis," *Robot. Comput. Integr. Manuf.*, vol. 18, no. 3–4, pp. 233–239, Jun. 2002, doi: 10.1016/S0736-5845(02)00014-5.

[5] D. Tiwari, M. Farnsworth, Z. Zhang, G. W. Jewell, and A. Tiwari, "In-Process Monitoring in Electrical Machine Manufacturing: A Review of State of the Art and Future Directions," *Proc. Inst. Mech. Eng. Part B J. Eng. Manuf.*, vol. 235, no. 13, pp. 2035–2051, Nov. 2021, doi: 10.1177/09544054211016675.

[6] A. Decner, M. Baranski, T. Jarek, and S. Berhausen, "Methods of Diagnosing the Insulation of Electric Machines Windings," *Energies*, vol. 15, no. 22. Multidisciplinary Digital Publishing Institute, p. 8465, 12-Nov-2022, doi: 10.3390/en15228465.

[7] N. Simpson, R. Wrobel, and P. H. Mellor, "Estimation of Equivalent Thermal Parameters of Impregnated Electrical Windings," *IEEE Trans. Ind. Appl.*, vol. 49, no. 6, pp. 2505–2515, Nov. 2013, doi: 10.1109/TIA.2013.2263271.

[8] R. Wrobel, S. J. Williamson, J. D. Booker, and P. H. Mellor, "Characterising the performance of selected electrical machine insulation systems," in *2015 IEEE Energy Conversion Congress and Exposition (ECCE)*, 2015, pp. 4857–4864, doi: 10.1109/ECCE.2015.7310345.

[9] Y. Guo, J. Soulard, and D. Greenwood, "A Time-efficient Test Rig for Thermal Characterisation of Electric Machines and Manufacturing Process Development," in *2019 Fourteenth International Conference on Ecological Vehicles and Renewable Energies (EVER)*, 2019, pp. 1–7, doi: 10.1109/EVER.2019.8813670.

[10] V. Mihaila, S. Duchesne, and D. Roger, "A Simulation Method To Predict The Turn-to-Turn Voltage Spikes in a PWM Fed Motor Winding," *IEEE Trans. Dielectr. Electr. Insul.*, vol. 18, no. 5, pp. 1609–1615, Oct. 2011, doi: 10.1109/TDEI.2011.6032831.

[11] P. A. Panagiotou, A. Lambourne, and G. W. Jewell, "Ex-situ Inspection of Concentrated Stator Coils by Means of Impedance Spectroscopy," *Int. Conf. Electr. Mach. ICEM 2022*, pp. 2331–2337, 2022, doi: 10.1109/ICEM51905.2022.9910588.

[12] D. Roger, S. Duchesne, S. Ait-Amar, and P. Notingher, "Turn-to-Turn Capacitance Used as an Indicator of Winding Insulation Aging," *Stud. in Appl. Electromagn. and Mech.*, vol. 34, no. IOS Press, 2010.

[13] J. Yang, J. Cho, S. Bin Lee, J.-Y. Yoo, and H. D. Kim, "An Advanced Stator Winding Insulation Quality Assessment Technique for Inverter-Fed Machines," *IEEE Trans. Ind. Appl.*, vol. 44, no. 2, pp. 555–564, Mar. 2008, doi: 10.1109/TIA.2008.916753.

[14] V. Madonna, P. Giangrande, W. Zhao, Y. Wang, H. Zhang, and M. Galea, "Insulation Capacitance as Diagnostic Marker for Thermally Aged, Low Voltage Electrical Machines," *22nd Int. Conf. Electr. Mach. Syst. ICEMS 2019*, Aug. 2019, doi: 10.1109/ICEMS.2019.8921657.

[15] I. Tsyokhla, A. Griffo, and J. Wang, "Online Condition Monitoring for Diagnosis and Prognosis of Insulation Degradation of Inverter-Fed Machines," *IEEE Trans. Ind. Electron.*, vol. 66, no. 10, pp. 8126–8135, Oct. 2019, doi: 10.1109/TIE.2018.2885740.

[16] P. A. Panagiotou, K. N. Gyftakis, N. Lophitis, M. D. McCulloch, and D. A. Howey, "Investigation of Traction Motor Windings' Insulation Capacitance at Switching Frequencies Under Accelerated Thermal Stress," in *2017 IEEE 11th International Symposium on Diagnostics for Electrical Machines*, Power Electronics and Drives (SDEMPED), 2017, vol. 2017-Janua, pp. 537–543, doi: 10.1109/DEMPED.2017.8062407.

[17] M. F. Shaikh, H. Lee, B. Battulga, S. Bin Lee, and G. C. Stone, "Offline Common-Mode Voltage Based Inverter-Embedded Groundwall Insulation Testing for Motors," *Int. Conf. Electr. Mach. ICEM 2022*, pp. 1823–1829, 2022, doi: 10.1109/ICEM51905.2022.9910839.

[18] P. Werynski, D. Roger, R. Corton, and J. F. Brudny, "Proposition of a New Method for In-Service Monitoring of the Aging of Stator Winding Insulation in AC Motors," *IEEE Trans. Energy Convers.*, vol. 21, no. 3, pp. 673–681, Sep. 2006, doi: 10.1109/TEC.2006.875465.

[19] E. M. Committee, IEEE Recommended Practice for Measurement of Power Factor Tip-Up of Electric Machinery Stator Coil Insulation, vol. 2000. 2001.